Eutectic Formation During Solidification of Ni-Based Single-Crystal Superalloys with Additional Carbon

FU WANG, DEXIN MA, and ANDREAS BÜHRIG-POLACZEK

γ/γ' eutectics' nucleation behavior during the solidification of a single-crystal superalloy with additional carbon was investigated by using directional solidification quenching method. The results show that the nucleation of the γ/γ' eutectics can directly occur on the existing γ dendrites, directly in the remaining liquid, or on the primary MC-type carbides. The γ/γ' eutectics formed through the latter two mechanisms have different crystal orientations than that of the γ matrix. This suggests that the conventional Ni-based single-crystal superalloy castings with additional carbon only guarantee the monocrystallinity of the γ matrix and some γ/γ' eutectics and, in addition to the carbides, there are other misoriented polycrystalline microstructures existing in macroscopically considered "single-crystal" superalloy castings.

DOI: 10.1007/s11661-017-4317-1

I. INTRODUCTION

CARBON is conventionally added to Ni-based equiaxed (EQ) and directional solidified (DS) superalloys to strengthen grain boundaries (GB) through the formation of carbides.[1] Due to the disappearance of GB in Ni-based single-crystal (SC) superalloy components, this element was eliminated in earlier-developed SC superalloys to increase incipient melting temperatures during the heat treatment process.[2] With the development of Ni-based SC superalloys, carbon has been reintroduced into Ni-based SC superalloys because it purifies the alloy melt,[3] reduces the extent of segregation of refractory elements,[4,5] impedes convection in the interdendritic regions and further alleviates the occurrence of freckle defects,[6] reduces the formation of surface scale on Ni-based SC castings[7] as well as strengthens any low-angle grain boundaries (LAGBs), which are often present in large SC components.[8] Despite these advantages, a small amount of MC-type carbides formed during solidification negates the local monocrystallinity of Ni-based SC components and is detrimental to the mechanical properties by acting as initiation sites of cracks thus leading to the component's final fracture.[1]

Due to the different orientations of carbides than that of the γ matrix, macroscopically defined SC castings of Ni-based superalloy with additional carbon can be microscopically considered as pseudo-SC components. During their solidification, multiple-phase transformations occur.[9–11] When the temperature of the superalloy melt decreases below its melting point, the γ phase having dendritic morphology primarily crystalizes from the melt. Following this, primary MC-type carbides precipitate from the melt. As the solidification proceeds, the γ dendrites coarsen and the MC-type carbides grow larger. During the final stage of the solidification, γ/γ' eutectics form from the remaining liquid in the interdendritic regions. Meanwhile, fine γ' particles precipitate from the γ matrix through solid-state phase transformation.

As one of the most important phases in as-cast Ni-based SC superalloys, the formation of the γ/γ' eutectics are significantly affected by the alloy's composition and the casting process. During the previous several decades, a large number of studies were conducted to investigate the morphological evolution, the size, and the volume fraction of the γ/γ' eutectics under different solidification conditions[12,13] as well as the internal microstructural formation of the γ/γ' eutectic.[14–19] However, the relationship of the nucleation behavior of the γ/γ' eutectics with γ dendrites, MC-type carbides, and the residual, interdendritic liquid has not been investigated. The purpose of this study is to explore the effect of the existing γ dendrites and MC-type carbides as well as the residual liquid on the γ/γ' eutectic formation in the Ni-based SC superalloy with additional carbon.

II. EXPERIMENTAL PROCEDURES

The superalloy CM247LC (Ni-0.094C-5.49Al-0.74-Ti-8.03Cr-0.5Mo-9.41Co-9.87W-2.9Ta-1.36Hf (wt pct)) was used in this investigation. During the experiment, ∅20 × 150 mm SC rods were placed in a

FU WANG, DEXIN MA, and ANDREAS BÜHRIG-POLACZEK are with the Foundry Institute, RWTH Aachen University, Intzestrasse 5, 52072 Aachen, Germany. Contact e-mail: darrel0112038@hotmail.com
Manuscript submitted June 4, 2017.
Article published online September 7, 2017

ceramic tube and raised into a vertical Bridgman-type laboratory furnace[20] chamber which was pre-heated to 1733 K (1460 °C). A section of the rod remained at this temperature for 15 minutes. The temperature of the melt, which was shielded using high-purity argon gas, was measured by lowering a thermocouple into this melt. The furnace temperature was held constant for 10 minutes to enable the temperature to homogenize. Following this, the tube was withdrawn from the chamber at a withdrawal rate of 0.2 mm min^{-1}. After withdrawing a definite solidification length, the tube was quickly removed from the furnace chamber and quenched in a water bath. The cooling curve was obtained from the measured temperature data. According to this curve, the thermal gradient at the liquid–solid interface was evaluated as 5.1 K (°C) mm^{-1}.

After quenching, the partially remelted and directionally solidified rod was longitudinally sectioned. The microstructural evolution was characterized by both sequentially studying transversally milled sections from the top to the bottom of the mushy zone as well as its longitudinal section. The material removed in each milling cycle varied from 0.05 to 0.2 mm. The etching solution used was 60 mL C_2H_5OH + 40 mL HCl + 2g ($Cu_2Cl{\cdot}2H_2O$). The microstructure was depicted using an Axioplan 2 optical microscopy. The concentrations of the alloying elements in MC-type carbides were determined by using energy dispersive X-ray analysis. Six carbides were examined. The crystallographic orientation relationships among the γ/γ' eutectics, γ dendrites, and MC-type carbides were analyzed by electron backscatter diffraction.

III. RESULTS AND DISCUSSIONS

Figure 1(a) depicts the morphology of the quenched mushy zone on the longitudinal section. Figure 1(b) through (d) shows the morphologies of MC-type

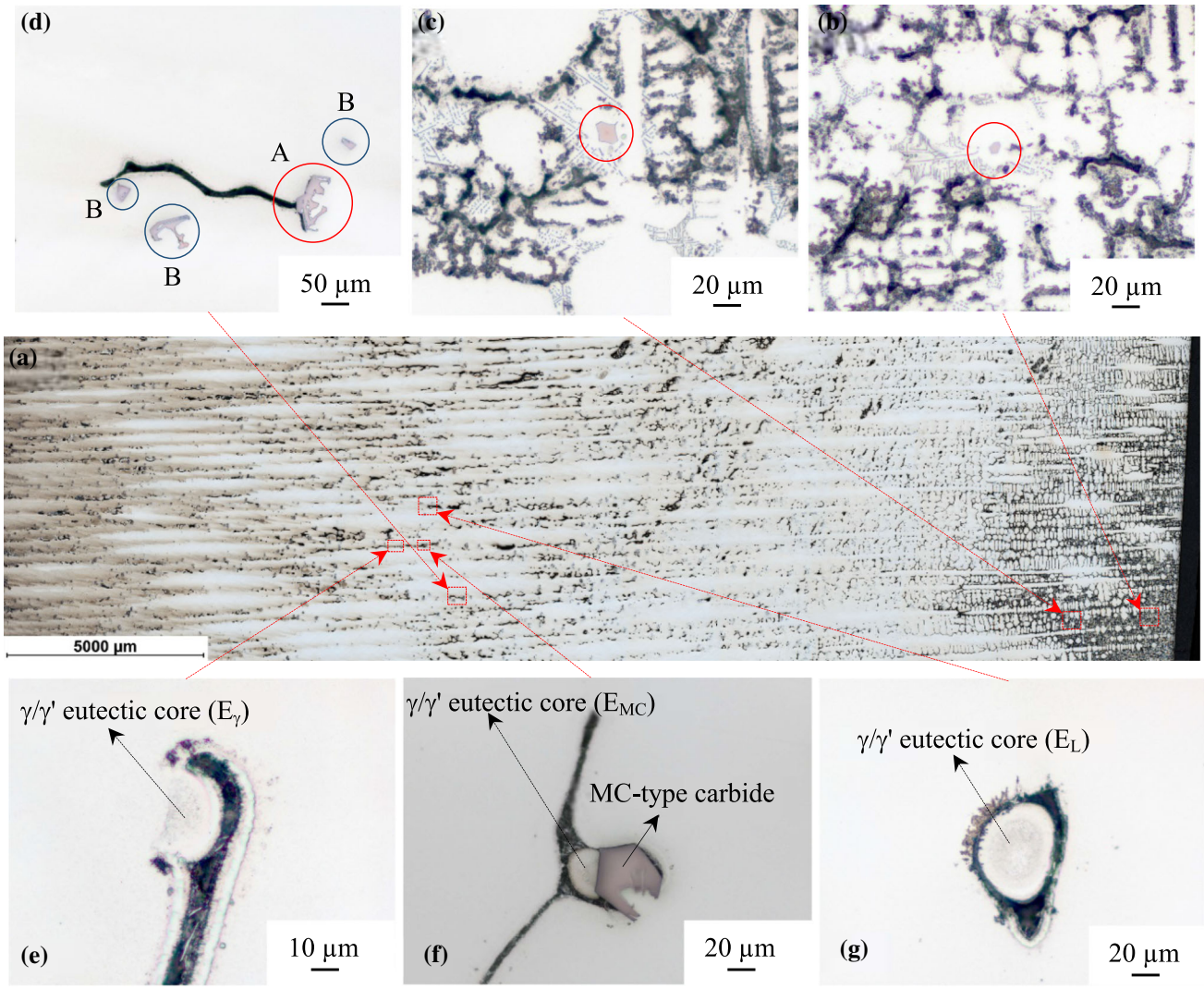

Fig. 1—Nucleating and growing processes of MC-type carbides and γ/γ' eutectics. The morphology of the quenched mushy zone (*a*); The morphology of MC-type carbides at different depths of the mushy zone (*b*) through (*d*); Different nucleation modes of γ/γ' eutectics (*e*) through (*g*).

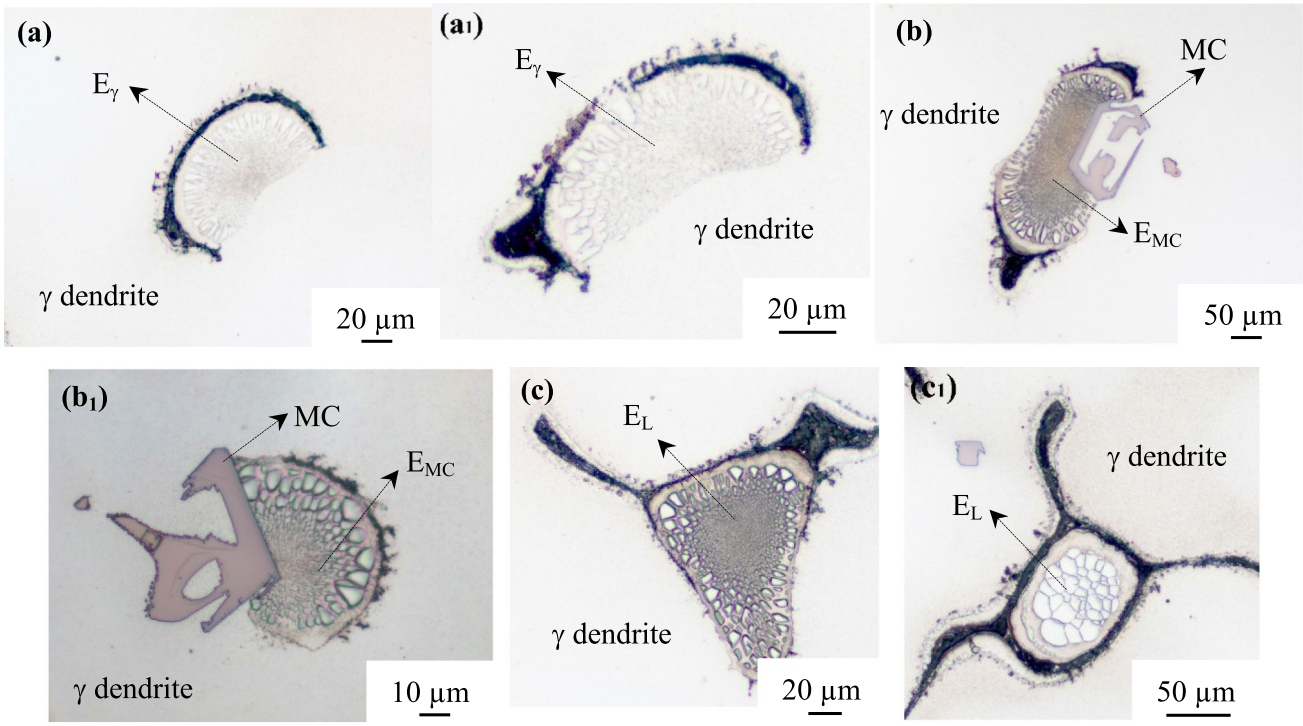

Fig. 2—Morphologies of well-developed γ/γ' eutectics in a transverse section derived from heterogeneously nucleated core on the γ dendrite (*a*, *a1*), heterogeneously nucleated core on the MC-type carbide (*b*, *b1*), and homogeneously nucleated core from the remaining liquid (*c*, *c1*).

Table I. The Concentrations (Wt Pct) of Alloying Elements (*i*) in MC-type Carbides $\left(C^i_{MC}\right)$ and Master Alloy $\left(C^i_{MC}\right)$ as Well as Their Specific Values (k^i)

Element *i*	C	Al	Ti	Cr	Mo	Co	W	Ta	Hf	Ni
C^i_{MC}										
1#	3.8	0.0	6.3	0.1	0.7	0.2	7.3	39.1	41.5	1.0
2#	2.5	0.2	8.7	0.4	0.8	0.3	7.7	66.7	10.8	1.8
3#	3.9	0.2	8.2	0.5	0.9	0.1	8.9	65.0	11.4	0.9
4#	3.6	0.1	6.5	0.2	0.4	0.3	5.4	58.	22.	2.1
5#	3.4	0.1	6.5	0.4	0.4	0.4	4.3	60.	21.	2.6
6#	3.1	0.1	6.8	0.4	0.6	0.4	5.0	61.1	19.2	3.3
Average	3.38	0.12	7.17	0.33	0.63	0.28	6.43	58.6	21.1	1.95
C^i_o	0.094	5.49	0.74	8.03	0.50	9.41	9.87	2.9	1.36	61.61
$k^i = C^i_{MC}/C^i_o$	36.0	0.022	9.7	0.041	1.26	0.030	0.65	20.2	15.5	0.031
MC-type carbides forming element	yes	no	yes	no	unclear	no	unclear	yes	yes	no

carbides at different depths in the mushy zone demonstrating the forming process of the MC-type carbides. As shown in Figure 1(b) at 0.66 mm from the dendrite tip, MC-type carbides precipitate directly from the liquid in the interdendritic regions ($L_1 \rightarrow MC + L_2$). At this position, the temperature is 3.4 K (°C) lower than the crystallization temperature of γ dendrites. With a further reduction in the temperature, MC-type carbides are becoming large, block-like, and anchor-like shapes, as shown in Figure 1(c) and (d). During the growth process, some MC-type carbides are completely enveloped by γ dendrites because of their transversal growth (Figure 1(d) (B)), whereas the remaining carbides are partially enclosed, as marked in Figure 1(d) (A).

With further decreases in temperature, γ/γ' eutectics precipitate from the remaining liquid in the interdendritic regions through the eutectic reaction ($L_2 \rightarrow \gamma/\gamma' + L_3$). The nucleation position of γ/γ' eutectics is approximately 18.8 mm from the dendrite tip where the temperature reduction at this point is 95.9 K (°C). Three types of nucleation modes of γ/γ' eutectics can be observed in Figure 1(e) through (f). A few γ/γ' eutectics heterogeneously nucleate on γ dendrites (E_γ) which was reported in the previous studies.[15,19,21,22] A number of γ/γ' eutectics homogeneously nucleate directly in the remaining liquid (E_L). A certain number of γ/γ' eutectics heterogeneously nucleate on MC-type carbides (E_{MC}). After nucleating, these γ/γ' eutectics grow three dimensionally in different directions until they meet the

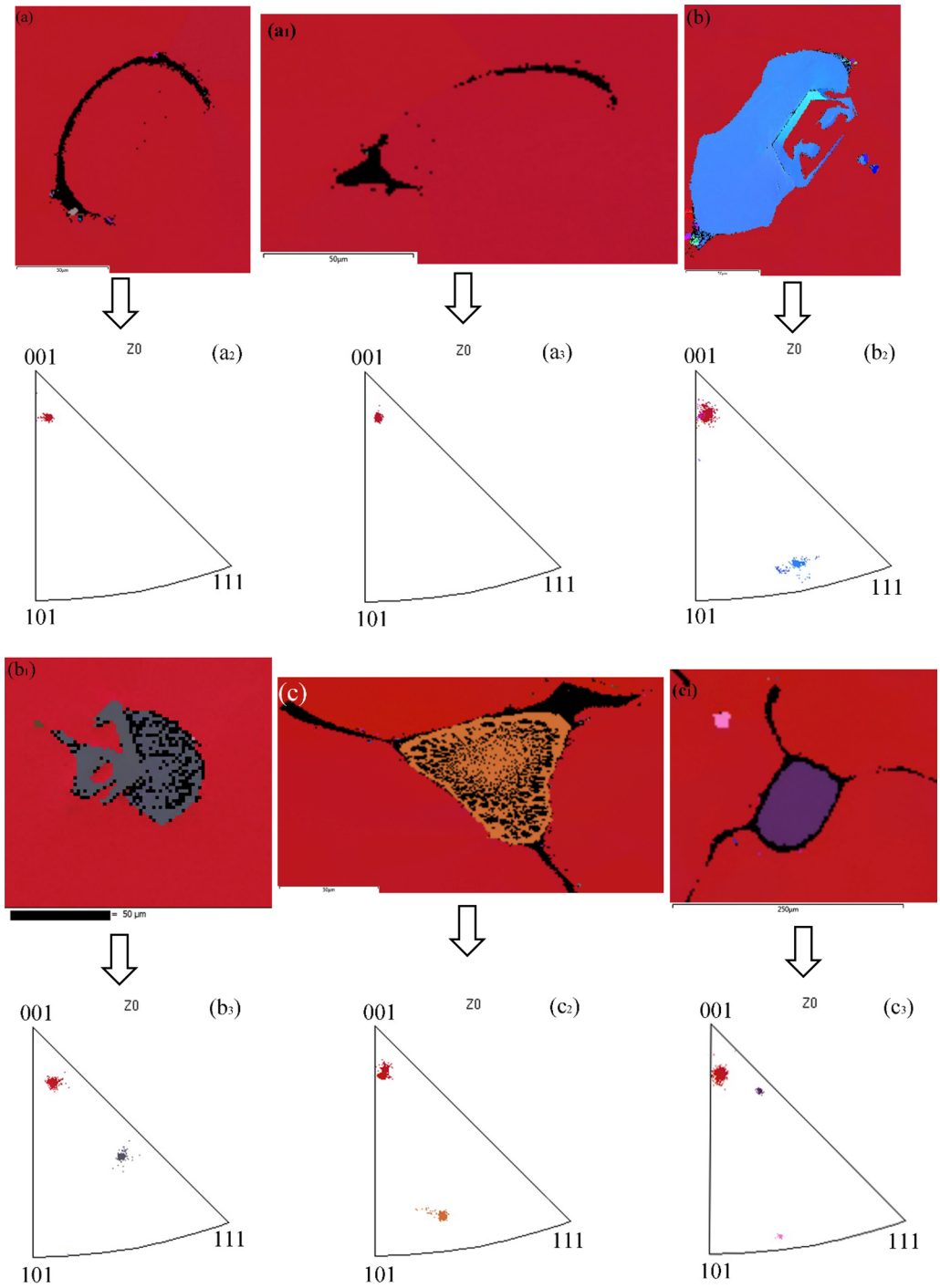

Fig. 3—EBSD mappings and inverse pole figures of the microstructures illustrated in Fig. 2. (*a*), (*a*$_1$), (*b*), (*b*$_1$), (*c*), and (*c*$_1$), respectively.

boundary of neighboring γ dendrites, as shown in Figure 2.

The concentrations of alloying elements (i) in MC-type carbides $\left(C^i_{\mathrm{MC}}\right)$ are listed in Table I. The specific values of the average concentrations of alloying elements (i) to their concentrations in the master $\left(C^i_{\mathrm{o}}\right)$ alloy, denoted as $k^i = C^i_{\mathrm{MC}}/C^i_{\mathrm{o}}$, are calculated to show the contribution of alloying elements to MC-type carbides formation.

It can be seen from Table I that the k^i values of C, Ta, Hf, and Ti are much greater than one. These are typical MC-type carbides forming elements. The values of Al, Ni, Co, and Cr are much less than one which suggests that these elements are not MC-type carbide forming elements. These alloying elements are rejected from MC-type carbides during their solidification. The k^i values of Mo and W are a little greater and a little less than one, respectively, which indicates that both of these

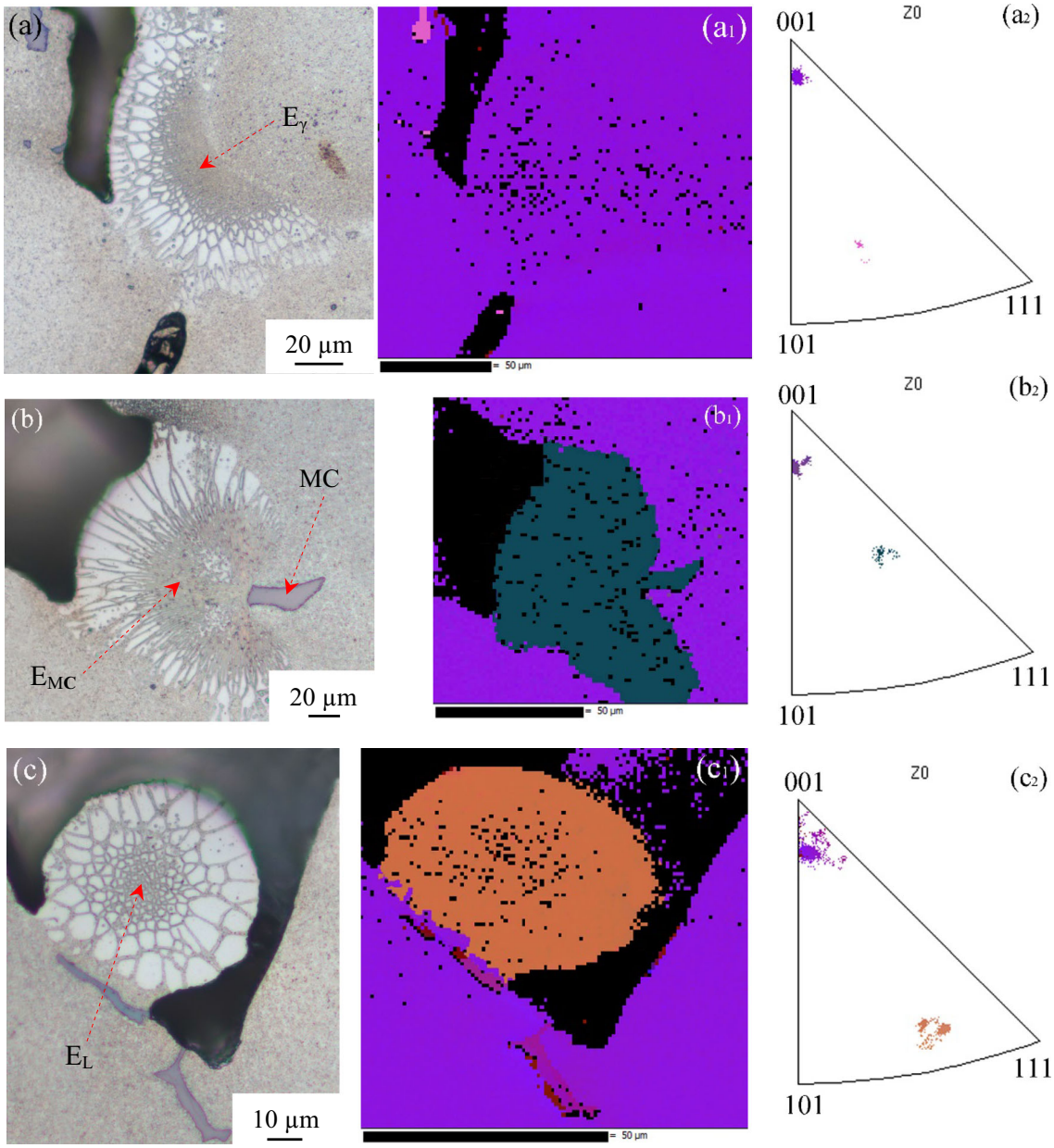

Fig. 4—Morphologies of the three types of γ/γ' eutectics found on a transversal section of SC CM247LC superalloy solidified at the withdrawal rate of 3 mm min^{-1} (*a*) (*b*) (*c*) and their EBSD mappings (a_1) (b_1) (c_1) as well as their inverse pole figures (a_2) (b_2) (c_2).

alloying elements make a small contribution to the MC-type carbides' formation.

Figure 3 shows EBSD mappings and inverse pole figures of the microstructures in a transverse section, which correspond to those in Figure 2. In this figure, orientation relationships can be found between γ/γ' eutectics and γ dendrites as well as the MC-type carbides subject to different nucleation modes. The γ dendrites are depicted as red, whereas the MC-type carbides and the γ/γ' eutectics are depicted as blue (Figure 3(b)) and dark gray (Figure 3(b_1)). The differences in the degree of misorientation between γ dendrites and γ/γ' eutectics are approximately 34 deg (Figure 3(b_2)) and 19 deg (Figure 3 (b_3)). This indicates that the MC-type carbide in this transverse section has the same crystallographic orientation as the γ/γ' eutectic upon which it is nucleated, whilst having a significantly different crystallographic orientations than the γ dendrite.

MC-type carbides are randomly and directly precipitated from the remaining liquid in the interdendritic region. Therefore, they have random crystallographic orientations, and their orientation is unaffected by the crystallographic orientation of γ dendrites. Since the γ/γ' eutectics nucleate on MC-type carbides, their crystallographic orientation is determined by a definite crystal plane of MC-type carbides. This kind of γ/γ' eutectic is unrelated to the γ dendrites' crystallographic orientation.

Figure 3(c) (c_1) demonstrates that the γ/γ' eutectics nucleated directly in the remaining liquid have different colors to the γ dendrites. This suggests that this type of

γ/γ' eutectics possesses a different crystallographic orientation to the γ dendrites. In terms of their inverse pole figures depicted in Figure 3(c_2) and (c_3), the differences in the degree of misorientation between γ dendrites and γ/γ' eutectics can reach about 31 and 6 deg. These eutectics randomly and directly nucleate from the remaining liquid at the final stage of the solidification process. Their crystallographic orientation is random, and is not influenced by the orientation of the γ dendrite. On the contrary, the γ/γ' eutectics nucleating on the γ dendrites have the same color as those γ dendrites (shown in Figure 3(a) and (a_1)). This indicates that they have the same crystallographic orientation (shown in Figure (a_2) and (a_3)). Since this kind of γ/γ' eutectics nucleates on a certain crystal plane of the γ dendrite, their orientation is determined by that γ dendrite. The EBSD results suggest that, apart from MC-type carbides, some local polycrystalline grains (E_L and E_{MC}) exist at the microscale in macroscopically considered Ni-based SC superalloy castings which affect the integrity of these SC castings.

The crystallization of solid phases starts with nucleation, which prefers to occur on the existing solid substrate thereby significantly reducing the nucleation energy. Prior to the γ/γ' eutectics' crystallization, γ dendrites, and MC-type carbides already exist in the mushy zone, where the γ dendrites occupy the vast majority of the volume and surface area fractions. More importantly, the γ and γ' phases in γ/γ' eutectics are homogeneous and coherent with the γ dendrite. For this reason, γ dendrites should be the best substrate for the γ/γ' eutectics' nucleation, as shown in Figures 1(e) and 2(a) and (a_1). In contrast to this, MC-type carbides possess smaller volume and surface area fractions, and exhibit a substantial difference in chemical properties to γ/γ' eutectics. In addition to this, more nucleation energy is required for γ/γ' eutectics' homogeneous nucleation directly in the remaining liquid. However, as shown in Figure 1, a certain number of γ/γ' eutectics still nucleate on MC-type carbides (E_{MC}) or directly from the remaining liquid (E_L) rather than on γ dendrites (E_γ).

During solidification of MC-type carbides, the alloying elements Al, Ni, Co, and Cr are rejected (shown in Table I), and then enrich and accumulate around MC-type carbides. Here, Al and Ni are the γ' phase's forming elements and Ni, Co, and Cr are the γ phase's forming elements. This situation creates good co-growing conditions for the γ and γ' phases. Particularly at a low withdrawal rate, the MC-type carbides are larger and can reject much more elements forming both the γ and the γ' phases during solidification. For this reason, the composition of the remaining liquid around MC-type carbides is liable to exceed the saturation level, and thus support the γ/γ' eutectic reaction to occur on the MC-type carbides.

A previous study[23] reported that the γ/γ' eutectic nucleation in the remaining liquid can occur on γ dendrites or directly from the liquid, which strongly depends on the local undercooling of the remaining liquid. Figures 1(g) and 2(c) and (c_1) show that the nucleation region of the γ/γ' eutectic precipitated directly in the remaining liquid has a triangular shape. This triangular region is formed by the neighboring γ dendrites. In contrast to the nucleation region of the γ/γ' eutectic nucleated on γ dendrites (shown in Figures 1(e) and 2(a) and (a_1)), more γ dendrites form this triangular region. During solidification of γ dendrites, more of the γ' phase forming elements (Al, Ti, Ta) accumulate in the triangular region. In addition to this, the γ phase forming elements (Cr, Co, W, Mo, Ni) and also the γ' phase forming element (Ni) still retain higher concentrations in the center of the triangle and cannot be quickly depleted by the growth of the surrounding γ dendrites. On the one hand, this concentration provides a fine, co-growing condition for both the γ and the γ' phases in the center of the triangular region. On the other hand, a larger local nucleation undercooling can be obtained in the remaining liquid in the center of the triangular region. For this reason, the γ/γ' eutectic can nucleate directly in the remaining liquid in the interdendritic region.

In this investigation, a lower withdrawal rate was used to achieve a relatively coarse as-cast microstructure such that γ/γ' eutectics nucleation can be clearly observed. To verify the three nucleation modes of γ/γ' eutectics under actual industrial casting conditions, a SC CM247LC superalloy was solidified using a withdrawal rate of 3 mm min^{-1}. Figure 4 shows that three nucleation modes of the γ/γ' eutectics (E_L, E_{MC}, and E_γ) can also be found in a transverse section, as marked in Figure 4. Using this withdrawal rate, the size of MC-type carbides is reduced. A fewer number of γ/γ' eutectics are nucleated on MC-type carbides than that at lower withdrawal rates.

At higher withdrawal rates, the total amount of the γ and γ' phase forming elements rejected from the refined MC-type carbides is reduced, and the enrichment of these elements around the carbides is alleviated. This weakens the co-growing chemical potential of the γ and γ' phases. For this reason, γ/γ' eutectic reactions on MC-type carbides are reduced.

The present investigation indicates that the macroscopically considered SC solidification of Ni-based superalloy with additional carbon only guarantees the monocrystallinity of γ dendrites and some γ/γ' eutectics. Besides MC-type carbides, there are a certain number of γ/γ' eutectics having different crystallographic orientations than the γ dendrites existing in the as-cast microstructure. Since γ/γ' eutectics constitute a considerable volume fraction (approximately 5 pct[24]) of the microstructure, they can greatly affect the SC integrity of the castings. Specifically, although the macroscopically defined SC castings of Ni-based superalloy with additional carbon eliminate the macro-defects, such as stray grains, freckles, silvers, and have a consistent γ dendrite growth orientation, they do not possess an entirely SC structure at the micro-level. The γ/γ' eutectics which have different orientations than the γ dendrites can act as micro-stray grains existing in the interdendritic regions. Even if γ/γ' eutectics can be partially or even completely dissolved during the subsequent solid-solution heat treatment, they can also serve as the core of recrystallization and grow into large stray grains. These grains degrade the high temperature performance of SC castings.

IV. CONCLUSIONS

In conclusion, during the final stage of solidification of Ni-based SC superalloy with additional carbon, three different nucleation modes of γ/γ' eutectics are found: nucleation on the existing γ dendrites, nucleation on the existing MC-type carbides, and those carbides which are partially enveloped by the γ dendrites, as well as nucleation directly in the remaining liquid. The γ/γ' eutectics nucleated through the latter two modes have different crystallographic orientations than the γ dendrites. This indicates that macroscopically defined SC castings of Ni-based superalloy with additional carbon still exhibit some other polycrystalline structures at a microscopic scale besides the carbides.

ACKNOWLEDGMENTS

This research was supported by German Research Foundation through Grant No. MA 2505/3-1.

REFERENCES

1. L. Liu, T. Jin, N. Zhao, X. Sun, H. Guan, and Z. Hu: *Mater. Sci. Eng. A*, 2003, vol. 361, pp. 191–97.
2. Y. Xu, Q. Jin, X. Xiao, X. Cao, G. Jia, Y. Zhu, and H. Yin: *Mater. Sci. Eng. A*, 2011, vol. 528, pp. 4600–07.
3. D. Duhl: *Superalloys, Supercomposites and Superceramics*, Academic Press, New York, 1989, p. 164.
4. M. Gell, D. Duhl, and A. Giamei: in *Superalloys*, J. Tien, S. Wlodek, H. Morrow, M. Gell, and G. Mauer, eds., AMS, Metals Park, OH, 1980, pp. 205–14.
5. S. Tin and T. Pollock: *Mater. Sci. Eng. A*, 2003, vol. 348, pp. 111–21.
6. S. Tin, T. Pollock, and W. King: in *Superalloys*, T. Pollock, R. Kissinger, R. Bowman, K. Green, M. McLean, S. Olson, and J. Scbirra, eds., TMS, Warrendale, PA, 2000, pp. 201–10.
7. S. Tin, T. Pollock, and W. Murphy: *Metall. Mater. Trans. A*, 2001, vol. 32A, pp. 1743–53.
8. J. Minalisin, J. Corrigan, G. Gratti, and R. Vogt: U.S. Patent 20020007877 A1, 2002.
9. F. Ross and K. O'hara: in *Superalloys*, R. Kissinger, D. Bye, D. Anton, A. Cetel, M. Nathal, T. Pollock, and D. Woodford, eds., TMS, Warrendale, PA, 1996, pp. 19–25.
10. L. Zheng, C. Gu, and Y. Zheng: *Scripta Mater.*, 2004, vol. 50, pp. 435–39.
11. Y. Liang, J. Li, A. Li, X. Pang, and H. Wang: *Scripta Mater.*, 2017, vol. 127, pp. 58–62.
12. N. D'Souza, H. Dong, M. Ardanani, and B. Shollock: *Scripta Mater.*, 2005, vol. 53, pp. 729–33.
13. F. Wang, D. Ma, J. Zhang, L. Liu, J. Hong, S. Bogner, and A. Bührig-Polaczek: *J. Cryst. Growth*, 2014, vol. 389, pp. 47–54.
14. F. Wang, D. Ma, J. Zhang, L. Liu, S. Bogner, and A. Bührig-Polaczek: *J. Alloy. Compd.*, 2014, vol. 616, pp. 102–09.
15. N. D'Souza and H. Dong: *Scripta Mater.*, 2007, vol. 56, pp. 41–44.
16. Y. Zhu, S. Zhang, L. Xu, J. Bi, Z. Hu, and C. Shi: in *Superalloys*, S. Reichman, D. D.uhl, G. Maurer, S. Antolovich, and C. Lund, eds., TMS, Warrendale, PA, 1988, pp. 703–12.
17. N. D'Souza, M. Lekstrom, H. Dai, B. Shollock, and H. Dong: *Mater. Sci. Technol.*, 2007, vol. 23, pp. 1085–92.
18. F. Wang, D. Ma, J. Zhang, S. Bogner, and A. Bührig-Polaczek: *Mater. Charact.*, 2015, vol. 101, pp. 20–25.
19. N. D'Souza and H. Dong: in *Superalloys*, R. Reed, K. Green, P. Caron, T. Gabb, M. Fahrmann, E. Huron, and S. Woodard, eds., TMS, Warrendale, PA, 2008, pp. 261–69.
20. N. Warnken, D. Ma, M. Mathes, and I. Steinbach: *Mater. Sci. Eng. A*, 2005, vols. 413–414, pp. 267–71.
21. F. Wang, D. Ma, and A. Bührig-Polaczek: *Mater. Charact.*, 2017, vol. 127, pp. 311–16.
22. N. Warnken: *J. Phase Equilib Diff.*, 2016, vol. 37, pp. 100–07.
23. A. Heckl, R. Rettig, S. Cenanovic, M. Göken, and R. Singer: *J. Cryst. Growth*, 2007, vol. 312, pp. 2137–44.
24. F. Wang, D. Ma, S. Bogner, and A. Bührig-Polaczek: *Metall. Mater. Trans. A*, 2016, vol. 47A, pp. 2376–86.